Synthesis of Cobalt Iron Oxide Doped by Chromium Using Sol-Gel Method and Application to Remove Malachite Green Dye

Ebtisam K. Alwan[1], Aqeel Mohhamed Hammoudi[2], Intessar K. Abd[3], Maryam O. Abd Alaa[4], Mohammed Nsaif Abbas[5*]

Abstract

In the current paper, the nanoparticles of cobalt iron oxide doped by chromium (CIC) of ($Cr_xCoFe_{2-x}O_4$) formula were prepared by sol-gel method using the nitrate salts of the elements composed of this nanomaterial. The characteristic properties of CIC nanoparticles prepared were determined using X-ray diffraction (XRD) and Fourier-transform infrared spectroscopy (FTIR) in addition to scanning electron microscopy (SEM) and also examination of the surface area (BET). These tests showed that the CIC nanoparticle prepared was in a pure phase, in addition to having various functional groups; moreover their structural framework includes multiple pores, which was the reason for the high surface area, reached to 223.36 $m^2.g^{-1}$. The prepared CIC nanoparticle was applied as an adsorbent to recover the malachite green dye from aqueous contaminated solutions in a batch mode adsorption unit and under different operating conditions. Designing factors used to determine the efficiency of the CIC as an adsorption media for the organic dye included the acidic function (pH), contact time and amount of nanomaterial CIC. The obtained practical results showed that the removal efficiency of the malachite green dye using CIC nanoparticle was 88.519% at 50 ppm of the initial concentration of the contaminated solution and that the percentage removal was directly proportional to the amount of adsorbent, contact time and acidic function.

Key Words: CIC, Nanoparticles, Malachite Green, Sol-gel Method, Adsorption, and Cationic Nitrite Salts.

DOI Number: 10.14704/nq.2021.19.8.NQ21110 **NeuroQuantology 2021; 19(8):32-41**

Introduction

Pollution of water resources and bodies is considered as one of the biggest issues facing the world today (Abbas *et. al.*, 2019). Water pollution can be defined as the change in the physical, chemical or biological properties of water so that it becomes unfit for drinking or for human use (Peirce *et. al.*, 1998). It can also be defined as the presence of undesirable substances in the water at levels above acceptable levels of health or aesthetics (Omer, 2019). Water pollutants may include organic matter, heavy metals, dyes, toxic substances (chemical, physical, or biological), sediments, and various microorganisms. In 2015, 20% of polluted water worldwide was treated, and in developing countries 70% of polluted industrial water is disposed of in an inappropriate way (Sharma and Bhattacharya, 2017).

Corresponding author: Mohammed Nsaif Abbas
Address: [1]Diyala University, College of Education of Pure Science, Iraq; [2]Directorate of Vocational Education, Department of Vocational education-Third Karaih, Iraq; [3]Diyala University, College of Education of Pure Science, Iraq; [4]Diyala University, College of Education of Pure Science, Iraq; [5*]Mustansiriyah University, College of Engineering, Environmental Engineering Department, Iraq.
[5*]E-mail: mohammed.nsaif.abbas@uomustansiriyah.edu.iq
Relevant conflicts of interest/financial disclosures: The authors declare that the research was conducted in the absence of any commercial or financial relationships that could be construed as a potential conflict of interest.
Received: 02 June 2021 **Accepted:** 06 July 2021

According to World Health Organization (WHO) anticipations, 50% of population in the world will live in areas suffering from water scarcity by 2025 (WHO, 2017). Therefore, finding new methods and efficient materials to treat polluted water and remove various contaminants from it is considered a very important matter, to meet the increasing demand for water associated with the increase in population density and also as a result of the continuous industrial and civilized development (Aljeboree, and Abbas 2019; Abbas *et. al.*, 2020). The choice of method for treating polluted water depends on the type of pollutant, the degree of contamination, the use of the water after treatment, and of course the cost of the treatment process (Helmer and Hespanhol, 1997). Currently, there are several methods used with different parameters for treating contaminated water (Abbas *et. al.*, 2021), including advanced oxidation (Garrido-Cardenas *et. al.*, 2020), sedimentation (Prasad, 2019), coagulation (Cui *et. al*., 2020), membrane (Madhura *et. al.*, 2018), evaporation (Li *et. al*., 2016), reverse osmosis (Jiang *et. al*., 2018), ozonation (Wei *et. al*., 2017), ultrasound waves (Fetyan and Attia, 2020), precipitation (Mbamba *et. al*., 2015), and adsorption (Abbas, 2015). Among the aforementioned methods, the adsorption is standing out as one of the best techniques used not only in water treatment but also can be used to treat crude petroleum (Ali *et. al.*, 2021) due to its ease, low cost and high efficiency (Alalwan *et. al.*, 2018). One of the most important adsorbents used in the treatment of water with adsorption technology is activated carbon (Alrazzak *et.al*; 2017; Maddodi *et. al.*, 2020), but due to its high manufacturing cost and its loss of between 10-15% of its weight at each regeneration process, this led researchers to find alternative materials for activated carbon despite its high efficiency (Abbas and Alalwan, 2019; Patawat *et. al*., 2020).

Among the materials that have proven their efficiency on a large scale during the last two decades in using as catalysts (Alminshid *et. al.*, 2021) or treating contaminated water by various types of wastes are nanomaterials that have been used in the treatment of water contaminated with heavy elements (Sarma *et. al*., 2019), organic materials (Alalwan and Alminshid, 2020) and dyes (Chatterjee *et. al*., 2020). Nanomaterials can be defined as that distinct class of advanced materials that can be produced with their dimensional scales or the dimensions of their internal particles ranging from 1 to 100 nm. The small sizes and scales of these materials have led to behavior different from the traditional large-sized materials whose dimensions exceed 100 nanometers, and to have very distinct qualities and characteristics (Hashim et. al. 2019; Mubarak *et. al*., 2021). Nanomaterials have characteristics that distinguish them from other ordinary materials, so the surface area of nanomaterials and the number of their atoms is greater than that of regular materials, which have the same chemical composition (Nandita *et. al*., 2021). The reason for this is that they are reduced to less than a hundred nanometers, and this gives them a remarkable chemical activity, so they are used as catalysts (Onishi, 2020). Nanomaterials also possess new physical properties as they are more rigid and durable, and their melting point decreases as their diameters decrease (Wadhawan *et. al*., 2020). As a result of these multiple specifications of nanomaterials, they find wide applications in several fields including: gas sensors, magnetic devices, water purification, medicine, catalysts, recharging batteries and as catalysts in the preparation of many chemicals and in the field of water treatment using adsorption technology on porous nanocomposites (Onishi, 2020). The oxides of nanomaterials that include iron (Ferrite) in their composition possess distinct chemical and physical properties, including excellent magnetic, large specific surface area, their surface possesses a large number of active sites, high chemical stability, ease of preparation and transformation into the desired shape, in addition to the possibility of modifying its surface or adding a functional group to it (Reddy and Yun, 2016). Therefore, it can find it on the list of materials that used as adsorbents; because it can be easily and quickly separated from solution after adsorption using an external magnetic field. After separating them, the pollutants can be removed and reused many times, and helps to reduce water purification costs (Wadhawan *et. al*., 2020). The present study includes three objectives: The first goal is to prepare cobalt oxide - iron doped with chromium nanoparticles by the sol-gel method using nitrate salts of the constituent elements of this substance. While the other aim is the characterization of the properties of this material through X-ray diffraction (XRD), Fourier transform infrared (FTIR) and scanning electron microscopy (SEM) in addition to determining its surface area using BET method. The last purpose is determining the optimum conditions and efficacy of the prepared substance when applied as an adsorbent media to recover the industrial dye malachite green

from contaminated aqueous solutions.

Methodology

The cobalt iron oxide doped by chromium nanoparticles (CIC) preparation of chemical formula ($Cr_xCoFe_{2-x}O_4$) where x=0.1 using sol-gel method is investigated. Three nitrate salts used as started material to prepare sol solution. Theses salts were cobalt nitrate ($Co(NO_3)_2.6H_2O$) of 97-99% purity supplied by IndiaMART company, Iron(III) nitrate ($Fe(NO_2)_3.9H_2O$) of 98% assay supplied by ITW Reagents and Chromium(III) nitrate ($Cr(NO_2)_3.9H_2O$) supplied by CS PharmChem Limited. Three solutions were prepared by weighing stoichiometric amounts from nitrites compounds aforementioned and dissolved using deionized water (DI water) prepared laboratory by Geno™ Type 2 Deionized Water System (Thomas Scientific). The salts were added gradually to the DI water (each one alone) with continuous stirring using glass rod (Stirring Rod Glass Paddle 150mm length and 6mm diameter (Pack of 10); Wiltronics) until dissolved all the salt's amount with minimum volume of DI water and obtain clear solution. After ended the dissolution process, the three solutions were mixed together in a 250 ml beaker (Pyrex® Vista™, Carolina Biological) and then added to it citric acid monohydrate ($C_6H_8O_7.H_2O$), ACS Reagent supplied by Thomas Scientific which represents the first complex agent which before adding the second complex agent which was ethylene diamine tetra acetic acid (EDTA) of minimum 99% assay supplied by IndiaMART, Technical Grade. The two complex agents were added by a stoichiometric amounts with the amounts of nitrate salts solutions by molar ratio of (1.5:1:1) (citric acid: EDTA: cations). To prepare gel, the evaporation method was used through heating the previously prepared sol solution using hot plate with magnetic stirrer (AREC Series, VELP Scientific, Inc.) to 75 ºC with heating rate of 5ºC/min. while the acidic function of the mixture was controlled using 0.1 M ammonia solution of 27.0-31.0 % w/w assay (supplied by PCCA Laboratories co., Ltd.) by adding rate 10 drop/min until pH was neutral. The heating process continued until the mixture converted to black and dense material which represents the gel. When the heating temperature reached to 150 ºC, the mixture converted to black ash, so the hot plate was shut down and the mixture left to cool at room temperature. After that the produced ash was crushed manually by laboratory porcelain mortar and pestle (mortar of height 9 cm and Ø 18.5 cm, while pestle of length 20.5 cm and Ø 5.5 cm) and then burned by muffle furnace (500×300×300 mm, LUWEI KSS-1200, EC21 China) using 100 ml capacity crucible with lid (High Tall Form Porcelain Crucible: 63mm rim diameter. 34mm outside diameter. 57mm height, Science Lab Supplies) at 600 ºC for 5 hours to get rid of remaining organic compounds and produce pure phase CIC nanoparticle powder which is considered the adsorbent media for removing malachite green dye from its aqueous solutions.

Characterization of Prepared Nanoparticles (CIC): to determine the characteristics properties of prepared Cobalt iron oxide doped by chromium (CIC) nanoparticles, four physical tests used which were X-ray diffraction (XRD), Fourier-transform infrared spectroscopy (FTIR), scanning electron microscopy (SEM), and **B**runauer–**E**mmett–**T**eller (BET) surface area.

X-ray Diffraction (XRD) test: The X-ray diffraction (XRD) device was used to identify the crystal structure of the CIC prepared nanoparticles (Gupta *et. al*., 2020). The highest peak was selected to calculate the size of the crystals using the Debye-Scherrer equation. The crystal axes and the density of the prepared material were also calculated using the following equations.

$$d_{hkl} = \frac{K\lambda}{B_{hkl}\cos\theta} \quad \ldots(1) \qquad d_{hkl} = \frac{a}{\sqrt{h^2+k^2+l^2}} \quad \ldots(2) \qquad D_{XRD} = \frac{MW.Z}{NV} \quad \ldots(3)$$

Where: d_{hkl}: is the crystallite size in the direction perpendicular to the lattice plane, hkl : are the Miller indices of the planes being analysed, K: is a numerical factor frequently referred to as the crystallite-shape factor ($K = 0.9$ In case of no information), λ: is the wavelength of the X-ray (which is for CuK_α=1.54051Å), B_{hkl}: is the width (full-width at half-maximum) of the X-ray diffraction peak in radians, θ: is the angle of Bragg, a : is the crystal axis and in cubic system ($a = b = c$) , D_{XRD} : is the density calculated according to XRD (g.cm^{-3}), MW: is the molecular weight of prepared CIC nanoparticles, Z: is the number of atoms per cell unit (for prepared CIC nanoparticles $= 8$), N : is Avogadro Number $= 6.0224 \times 10^{23}$ mol^{-1} and V: is the volume of cell unit $= a^3$.

Fourier-transform infrared spectroscopy (FTIR): This test was used to determine the functional groups on the surface of the prepared

CIC nanoparticle before and after its use as a media for malachite green dye adsorption (Adeyi *et. al*., 2019). To achieve this goal, the studied specimens were prepared (before and after adsorption) by grinding them well until the diameter of the granule is <0.5 mm and then mixing it with the powder of reference material in a shaker (ShakIR, Super shake and Pellet making, PIKE Technologies) for 20 seconds, with a ratio of 1:35 and at a temperature of 20±1ºC. Potassium bromide (KBr) powder was used as a reference material, thus 23 mg of this powder put in the sample port via potassium bromide cell of 32×3 mm. All spectra were recorded using (FTIR Shimadzu 8400s) device within the range between 4000-400 cm^{-1}, the spectra obtained were analyzed and the functional groups were concluded comparing with the reference data for the wavelengths.

Scanning Electron Microscopy (SEM): The purpose of using a scanning electron microscope is to recognize the structural composition of CIC nanoparticles before and after malachite green dye adsorption. This goal can be carried out by creating an enlarged image of the tested specimens with a magnification power that is superior to other conventional optical microscopes. Therefore, the SEM depends on the formation of the magnified image on the use of electrons instead of light waves. The specimens to be examined by the SEM are prepared with special accuracy and care to withstand and resist the air space inside the electron microscope. Specimens are dried with a special technique to avoid damage to the sample, and then coated with a thin layer of gold by a spray coating machine (HOMAG SPRAYTEQ S-100) so that the specimen has ability to electrical conductivity, thus, the specimen becomes ready for analysis by SEM device. The specimen is placed inside a column of air in a microscope through an airtight plug and exposed to a high-energy beam of electrons. A group of scanning magnetic coils is founded near the bottom of the column that moves the concentrated beam of electrons over the specimen to be tested back and forth row by row until the whole specimen is covered. The final image is formed according to the number of electrons released from each point on the specimen surface, and thus the image is created completely simulating and identical to the specimen. The CIC specimens prepared were tested using a scanning electron microscope (FEI NOVA NanoSEM 450) with operating conditions of HV 10 kV, WD 5.1 mm, mag 25,000×, ETD detector and Free-Field lens mode.

BET Surface Area Measuring: The surface area is considered as one of the most important operational characterizations that should be measured for any catalyst or adsorbent material. Therefore, this important property was measured for the CIC nanoparticles prepared in this study using Quantachrome, Qsurf 9600 Thermo Finnegan Co., USA device, depending on physical adsorption-desorption for nitrogen gas at constant temperature which were the boiling point of liquid N_2 (-77K). Initially, the specimens were subjected for evacuating or off-gassing process. This step was conducted by weighing 1 gram of CIC and heating to 473.15 K using (Lindberg/Blue M™-Thermo Scientific™) vacuum oven for four continuous hours to remove any moisture from the specimens before testing process. The measuring of surface area of any material is based on the BET theory (Stephen Brunauer, Paul Hugh **E**mmett, and Edward **T**eller) which considered as extension for Langmuir theory through determining the point that covered by monomolecular layer of adsorbed gas on the powder surface. The gas is frequently being nitrogen for most solid materials. But the application of BET equation restricted by limited area which is often the first part of adsorption isotherm usually between 0.05 < (P/P°) < 0.35. The surface area can be calculated using the mathematical expression described in Equation (4):

$$\frac{1}{Q\left[\left(\frac{P^{\circ}}{P}\right)-1\right]}=\frac{1}{CQ_m}+\frac{C-1}{CQ_m}\left(\frac{P}{P^{\circ}}\right) \qquad (4)$$

Where P and P° are the equilibrium and the saturation pressure of adsorbates at the temperature of adsorption respectively, (P/P°) is the relative pressure, Q is the adsorbed gas quantity at STP ($g.g^{-1}$), and Q_m is the monolayer adsorbed gas quantity at STP ($g.g^{-1}$). C is the constant of BET equation related with the adsorption heat.

From the experimental results obtained and by plotting a straight line between $1/(Q[(P^{\circ}/P)-1])$ on y-axis vs (P/P°) on x-axis. The slop and intercept can withdraw which represent monolayer adsorbed quantity (Q_m) and constant (C).

Adsorption Experiments

Preparation of Malachite Green dye Stock Solution: the stock solution of malachite green dye of (C.I. 42000) supplied by (Alliance Organics LLP- Malad West, Mumbai, Maharashtra, India) was

prepared by dissolving exactly 1,000 mg in one liter of laboratory prepared double distilled water using water distillation unit (GFL-2012). By this procedure, every milliliter of prepared solution containing 1 mg of malachite green dye. So the concentration of produced solution is 1,000 ppm.

Calibration Curve: the maximum wavelength of dye (λ_{max}) was determined via constant concentration of malachite green dye which was (10 ppm). The wavelength was changing within the range of 610-620 nm by series of laboratory experiments. The absorbance of each wavelength was calculated using spectrophotometer device (UV-1800-Shimadzu/Japan) and plotted in **Figure 1** below. It is noticed that the value of maximum absorbance was 0.925 obtained at wavelength of 617 nm, which is the wavelength that selected to prepare the calibration curve of malachite green dye shown in **Figure 2**.

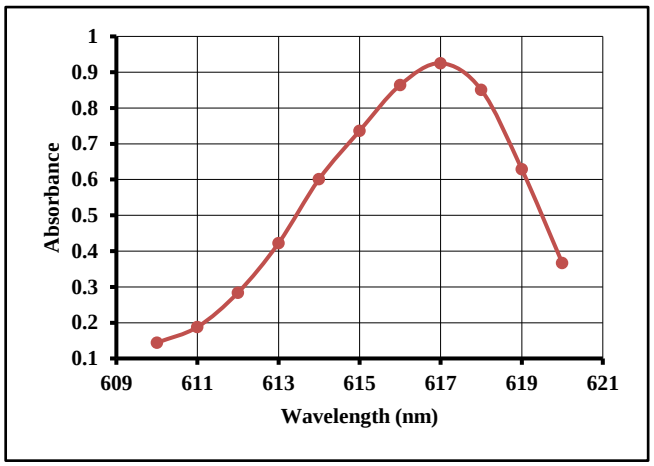

Figure 1. Changing of Wavelength with Absorbance for Malachite Green Dye

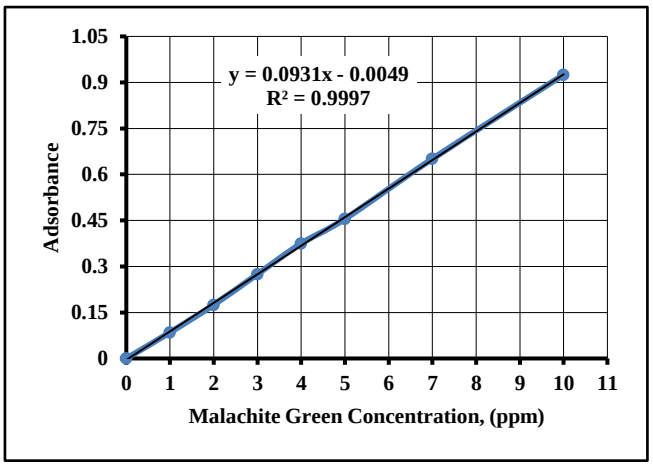

Figure 2. Calibration Curve of Malachite Green Dye using UV-Spectrophotometer

Batch Mode Adsorption Unit Used: The adsorption experiments of malachite green dye using CIC nanoparticles was performed by batch adsorption unit. The particular concentration of malachite green dye was prepared by diluted the required amount of stock solution using low of dilution. To detect the optimum operating conditions which achieve the maximum removal efficiency, the adsorption of malachite green dye was studied at different design parameters of acidic function (pH), contact time and CIC adsorbent dose which were varied between (1-9), (0.2-2.5) h and (0.1-1) g respectively. The values of initial concentration, agitation speed and temperature were kept constant at 50 ppm, 300 rpm and laboratory temperature (i.e. 25±2 ºC). To control the acidic function, prepared solutions of 0.1 N 98.9% assay sodium hydroxide (NaOH) supplied by (Fisher Scientific, Indian origin) and 0.1 N 31% hydrochloric acid (HCl) purchased from (Shijiazhuang Xinlongwei Chemical Co., LTD) were used. The experiments of adsorption was carried out by putting 100 ml of 50 ppm malachite green solution of specific pH value in a sealed conical flask of 150 ml (Pyrex® Borosilicate glass with glass stopper) and then the conical flasks were batched in shaker device (Stuart orbital shaker Model SSL1, 335×335 mm platform, speed accuracy ±2%). The experiment was started by fixing the speed and finished when the time period ended. The solution was filtered using vacuum filtration apparatus (JOANLAB VP-10L) and the CIC adsorbent media was extracted. The remaining concentration of malachite green dye in the treated solution was detected using UV-spectrophotometer device with calibration curve assist. The % removal of day and the adsorption capacity of CIC nanoparticle were calculated using Equations 5 and 6 respectively.

$$\%R = \frac{C_{in} - C_{out}}{C_{in}} \times 100 \quad \ldots (5)$$

$$q = \frac{V}{w}(C_{in} - C_{out}) \quad \ldots (6)$$

Where: $\%R$ is the removal efficiency of malachite green dye, C_{in} and C_{out}: are the initial and final concentration of malachite green dye respectively measured by (ppm), q: is the CIC capacity to adsorb the malachite green dye expressed in (mg/g), V: is the volume of solution measured by (L), w: is the amount of CIC used.

Results and Discussion

Morphology of CIC Nanoparticles Prepared

X-ray diffraction: The results obtained from XRD test that the prepared cobalt iron oxide doped by chromium nanoparticles has pure single phase as shown in **Figure 3**. This figure also refer that the ray diffraction pattern includes eight distinct peaks at Bragg angle (2θ) which were 28.76º , 34.98º , 40.66º , 43.26º , 55.04º , 59.75º , 65.30º , and 78.84º . These peaks related with the Miler indexes (220), (311), (222), (400), (422), (511), (440), and (533) respectively. By comparing the XRD spectrum obtained with standard files, it was found to be highly compatible with the spectrum of XRD model of cobalt-iron oxide ($CoFe_2O_4$) of a cubic crystal structure according to JCPDS no. 22-1086 as shown in **Table 1**.

Table 1. XRD properties of CIC nanoparticles prepared and standard

Sample	a (Å)	V (Å^3)	D_{XRD} (g.cm^{-3})
Prepared	8.3652	585.365	5.3155
JCPDS no. 22-1086 **(Stein *et. al.*, 2018)**	8.3919	590.99	5.274

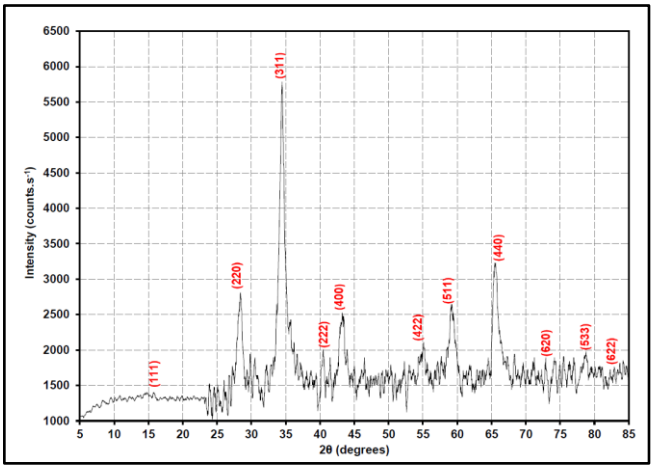

Figure 3. XRD of Prepared CIC nanoparticles

Fourier-transform infrared spectroscopy (FTIR): It's obvious from the obtained results of FTIR test elucidate by **Figure 4** that the CIC nanoparticles prepared has distinct absorbance band at 590.22, 883.40, 1154.33, 1651.07, 2914.09, and 3415.15 cm^{-1} which represents the bonds of Fe-O, aromatic C-H, C-O, C=N, C=H, and alcoholic O-H respectively. While **Figure 5** demonstrate that the CIC nanoparticles shows some wavenumber deviations as well as the disappearance of other wavenumbers from the shape after adsorption. This result can be explained by the fact that these active groups that appear in the wavenumbers have disappeared or decreased significantly due to the adsorption of the malachite green dye molecules, which means that the prepared CIC nanoparticles has perfect efficiency for dye adsorption.

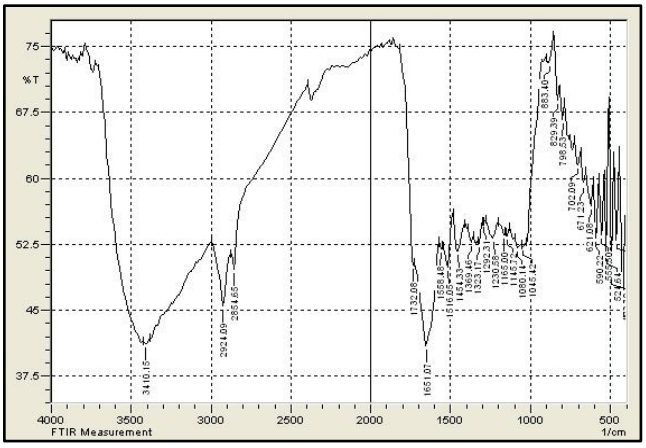

Figure 4. FTIR of Prepared CIC Nanoparticles Before Adsorption of Malachite Green Dyes

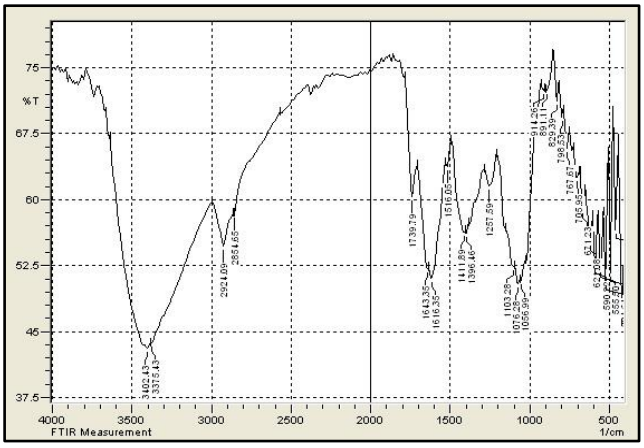

Figure 5. FTIR of Prepared CIC Nanoparticles After Adsorption of Malachite Green Dyes

Scanning Electron Microscopy (SEM): **Figure 6** show the SEM image of prepared cobalt iron oxide doped by chromium nanoparticles before and after adsorption of malachite green dye respectively. **Figure 6** exhibits that the surface of prepared CIC nanoparticles before adsorption contains clear pores and consistent particles in their sizes. While **Figure 7** elucidates that the pores have nearly faded and the sizes of nanoparticles have become distinctly different as a result of particles unification which may be attributed to malachite green dye adsorption. This confirms the results

concluded by the FTIR test that the prepared CIC nanoparticle is highly effective in adsorption of dyes.

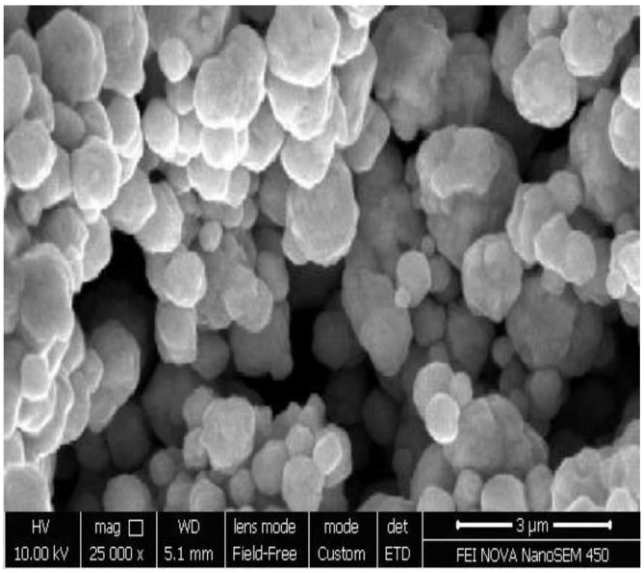

Figure 6. SEM of Prepared CIC Nanoparticles Before Adsorption of Malachite Green Dye

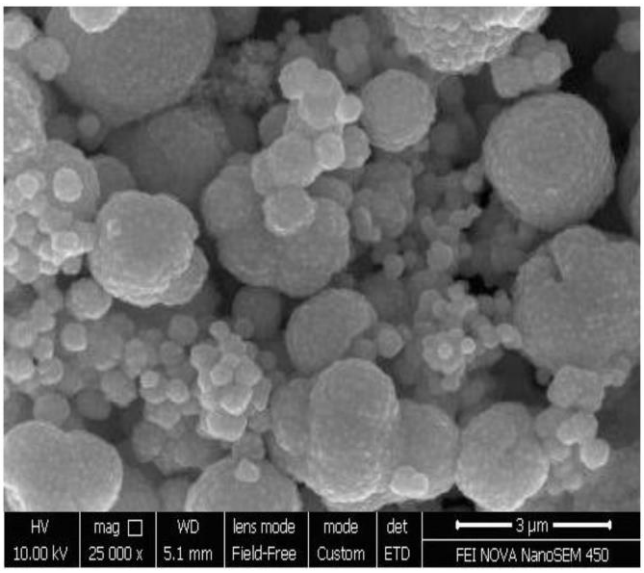

Figure 7. SEM of Prepared CIC Nanoparticles After Adsorption of Malachite Green Dye

Adsorption of Malachite Green Dye

Behavior of Acidic Function: The pH of the dye solution is one of the serious factors affecting the adsorption process, because it affects both the chemical composition of the dye molecules as well as the surface properties of the adsorbent. To comprehend the behavior of this parameter, the pH of adsorption process using prepared CIC nanoparticles was varied between (1-9), keeping other variables constant at optimum values. **Figure 8** shows the effect of acidic function on the efficiency of malachite green dye removal from aqueous solutions. It is noticed from the aforementioned figure that the relationship is direct between the removal efficiency and the pH, so the higher removal efficiency achieved at the higher pH, and vice versa. The percentage removal of malachite green dye is raises from 14.048% to 88.519% when the pH increased from 1 to 6 respectively. The reason for this result is that malachite green is classified as a basic (cationic) dye and gives positively charged ions when dissolved in water. Therefore, at low values of the acidic function, the surface of the adsorbent material (CIC) will be positively charged due to the increase in the number of positive hydrogen ions H^+ in the solution. As a result, the repulsion between the positively charged adsorbent surface and the positively charged malachite green dye will increase, which in turn will lead to lower both the dye removal percentage and the amount of adsorbent. This explains the low amount of dye adsorbed and consequently the lower values of removal at an acidic function of 1. While at values of the acidic function that exceed 6, the removal efficiency will rise sharply and reach the ideal value of 100%, due to the occurrence of dye precipitation at the bottom of the flask, meaning that the removal will occur as a result of the precipitation and not due to the adsorption process. Thus, the optimal value of the acidic function of malachite green adsorption is 6.

Behavior of Contact Time: The contact time between the adsorbent and the adsorbate is considered as a vital condition affecting the adsorption process of any substance. Therefore, the effect of the contact time, which ranged between 0.2-2.5 hours, on the percentage of malachite green dye removal using CIC nanoparticles was studied by fixing other design variables at the optimum values. As is evident from the **Figure 9**, the efficiency of removing malachite green dye increases with contact time increase, starting from the lowest value and reaching the highest value of 88.519% at 1.75 hours. Increasing the contact time means increasing the chance of the dye molecules adsorption at the active sites in the adsorbent surface, and this leads to decrease the dye concentration in the solution and thus increase the percentage of removal. After exceeding the time 1.75 hours, it is noticed that the removal efficiency will remain constant. The reason for this is due to

the saturation state which occurs at the active sites under used operational conditions. Therefore, 1.75 hours represents the ideal time to reach the optimum removal efficiency of malachite green dye from polluted aqueous solutions.

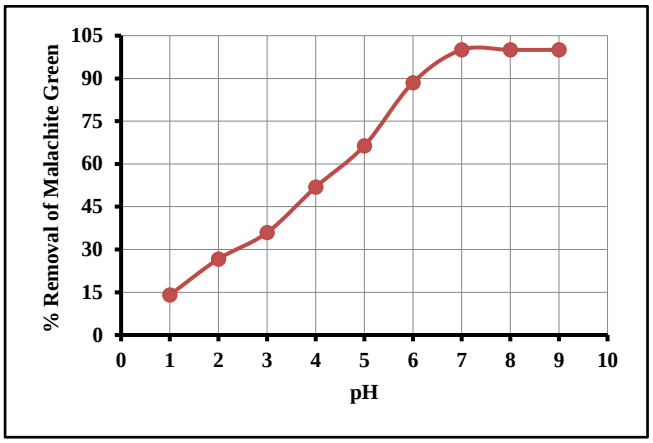

Figure 8. pH Behavior on % Removal of Malachite Green Dye using Prepared CIC Nanoparticles

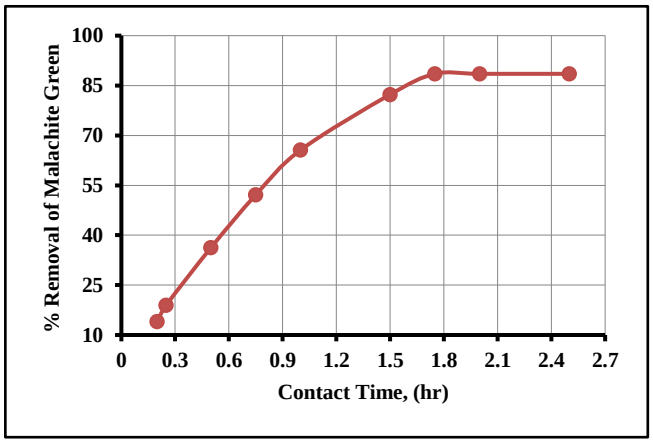

Figure 9. Contact time Behavior on % Removal of Malachite Green Dye using Prepared CIC Nanoparticles

Behavior of Adsorbent Dose: **Figure 10** shows the dose of adsorbent (prepared CIC nanoparticles) behavior effect on the efficiency of removing the malachite green dye from the polluted aqueous solutions. **Figure 10** demonstrates that increasing the removal percentage is achieved by increasing the amount of CIC nanoparticles and that the relationship between them is a direct relationship. The increasing of active sites number is achieved by increasing the amount of adsorbent, because CIC has a constant surface area per unit mass, which means increasing the functional groups that can adsorb the particles of malachite green dye from the aqueous solution and this leads to increase in the efficiency of treatment. It is also noticeable from the aforementioned figure that the removal efficiency increases gradually from minimum value of 14.048% to maximum value of 88.519% at 0.1g and 0.7g, respectively, after which the removing percentage remains constant and does not change. This result may be attributed to the saturation situation of the active sites on the surface of CIC, which does not allow the adsorption of more dye molecules from the contaminated solution. Therefore, 0.7g represents the optimum amount of prepared CIC nanoparticles to achieve the best treatment efficiency of the aqueous solution contaminated with malachite green dye.

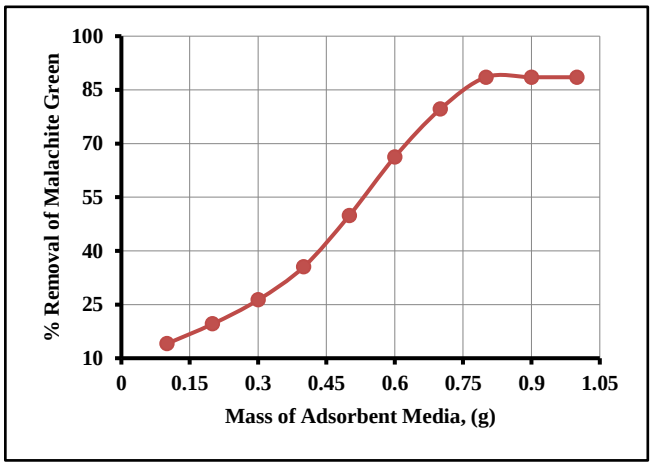

Figure 10. Prepared CIC Nanoparticles Amount Behavior on % Removal of Malachite Green Dye using

Conclusions

this study is dealt with the preparation of cobalt iron oxide doped by chromium (CIC) nanoparticles of chemical formula $Cr_xCoFe_{2-x}O_4$ where x=0.1, by sol-gel method and using the nitrate salts of the elements that formed this nanoparticle. The morphological tests were carried out for the prepared CIC nanoparticles, as the results of the FTIR analysis showed that it possesses multiple functional groups such as N – H, O – H, C – C, C – O and C – H. While SEM test demonstrate that the CIC nanoparticles of small ball form, connected with each other and have a clear porous structure surface. Moreover, XRD spectrum confirms that the prepared CIC nanoparticles have a pure single phase identical with $CoFe_2O_4$. Finally, the measured surface area of prepared CIC was 223.36 $m^2.g^{-1}$

according to BET test based on adsorption-desorption of nitrogen. CIC nanoparticles exhibit high ability to use as adsorbent media to remove malachite green dye from contaminated aqueous solution at various operating parameters. The maximum efficiency of adsorption process excessed 88% at initial concentration, pH, agitation speed, contact time and temperature of 50 ppm, 6, 300 rpm, 2.5 h, and laboratory temperature, while the optimum dose of CIC nanoparticle was 0.7 g. Thus, the prepared CIC nanoparticle is considered as active adsorbent to treat polluted wastewater.

References

Abbas MN, Alalwan HA. Catalytic Oxidative and Adsorptive Desulfurization of Heavy Naphtha Fraction. *Korean Journal of Chemical Engineering* 2019; 12(2): 283-288. https://doi.org/10.9713/kcer.2019.57.2.283

Abbas MN, Ali ST, Abbas RS. Rice Husks as a Biosorbent Agent for Pb^{+2} Ions from Contaminated Aqueous Solutions: A Review. *Biochemical and Cellular Archives* 2020; 20(1): 1813-1820. https://doi.org/10.35124/bca.2020.20.1.1813

Abbas MN, Al-Tameemi IM, Hasan MB, Al-Madhhachi AT. Chemical Removal of Cobalt and Lithium in Contaminated Soils using Promoted White Eggshells with Different Catalysts. *South African Journal of Chemical Engineering* 2021; 35: 23-32. https://doi.org/10.1016/j.sajce.2020.11.002

Abbas MN. Phosphorus removal from wastewater using rice husk and subsequent utilization of the waste residue. *Desalination and Water Treatment* 2015; 55(4): 970-977. https://doi.org/10.1080/19443994.2014.922494

Adeyi AA, Jamil SNAM, Abdullah LC, Choong TSY. Adsorption of Malachite Green Dye from Liquid Phase Using Hydrophilic Thiourea-Modified Poly (acrylonitrile-co-acrylic acid): Kinetic and Isotherm Studies. *Journal of Chemistry* 2019; 4321475: 14. https://doi.org/10.1155/2019/4321475

Alalwan HA, Abbas MN, Abudi ZN, Alminshid AH. Adsorption of thallium ion (Tl^{+3}) from aqueous solutions by rice husk in a fixed-bed column: Experiment and prediction of breakthrough curves. *Environmental Technology and Innovation* 2018; 12: 1-13. https://doi.org/10.1016/j.eti.2018.07.001

Alalwan H, Alminshid A. An in-situ DRIFTS study of acetone adsorption mechanism on TiO_2 nanoparticles. *Spectrochimica Acta Part A*: *Molecular and Biomolecular Spectroscopy* 2020; 229. https://doi.org/10.1016/j.saa.2019.117990

Ali GAA, Abbas MN. Atomic Spectroscopy Technique Employed to Detect the Heavy Metals from Iraqi Waterbodies Using Natural Bio-Filter (*Eichhornia crassipes*) Thera Dejla as a Case Study. *Systematic Reviews in Pharmacy* 2020; 11(9): 264-271.

Ali GAA, Ibrahim SA, Abbas MN. Catalytic Adsorptive of Nickel Metal from Iraqi Crude Oil using non-Conventional Catalysts. *Innovative Infrastructure Solutions* 2021; 6(7): 9 https://doi.org/10.1007/s41062-020-00368-x

Aljeboree AM, Abbas AS. Removal of Pharmaceutical (Paracetamol) by using CNT/ TiO2 Nanoparticles. *Journal of Global Pharma Technology* 2019; 11(1): 199-205.

Alminshid AH, Abbas MN, Alalwan HA, Sultan AJ, Kadhom MA. Aldol condensation reaction of acetone on MgO nanoparticles surface: an in-situ drift investigation. *Molecular Catalysis* 2021; 501: 111333. https://doi.org/10.1016/j.mcat.2020.111333

Alrazzak NA, Aowda SA, Atiyah AJ. Removal Bismarck Brown G dye from aqueous solution over a composite of triazole-polyvinyl chloride polymer and zinc oxide. *Oriental Journal of Chemistry* 2017; 33(5): 2476-2483.

Chatterjee S, Guha N, Krishnan S, Singh AK, Mathur P, Rai DK. Selective and Recyclable Congo Red Dye Adsorption by Spherical Fe_3O_4 Nanoparticles Functionalized with 1,2,4,5-Benzenetetracarboxylic Acid", *Scientific reports* 2020; 10(1). https://doi.org/10.1038/s41598-019-57017-2

Cui H, Huang X, Yu Z, Chen P, Cao X. Application progress of enhanced coagulation in water treatment. *RSC Advances* 2020; 10(34): 20231-20244. https://doi.org/10.1039/D0RA02979C

Fetyan NAH, Attia TMS. Water purification using ultrasound waves: application and challenges. *Arab Journal of Basic and Applied Sciences* 2020; 27(1): 194-207. https://doi.org/10.1080/25765299.2020.1762294

Garrido-Cardenas JA, Esteban-García B, Agüera A, Sánchez-Pérez JA, Manzano-Agugliaro F. Wastewater Treatment by Advanced Oxidation Process and Their Worldwide Research Trends. *International Journal of Environmental Research and Public Health* 2020; *17*(1). https://doi.org/10.3390/ijerph17010170

Gupta H, Rai SK, Kuchhal P, Anand G. Characterization and experimental investigation of rheological behavior of oxide nanolubricants. *Particulate Science and Technology* 2021; 39(6): 651-656. https://doi.org/10.1080/02726351.2020.1792018

Hashim FS, Alkaim AF, Mahdi SM, Alkhayatt AHO. Photocatalytic degradation of GRL dye from aqueous solutions in the presence of ZnO/Fe2O3 nanocomposites. *Composites Communications* 2019; 16: 111-116.

Helmer R, Hespanhol I. *Water pollution control: a guide to the use of water quality management principles*. CRC Press 1997.

Jiang L, Tu Y, Li X, Li H. Application of reverse osmosis in purifying drinking water. *4th International Conference on Energy Materials and Environment Engineering* (*ICEMEE*) 2018; 38 (E3S Web of Conferences). https://doi.org/10.1051/e3sconf/20183801037

Li H, Wang H, Liu Q, Tan Y, Jiang N, Lin Y. Evaporation process for treating high-salinity industrial wastewater at low temperatures and ambient pressure. *Desalination and Water Treatment* 2016; 57(56): 27048-27060. https://doi.org/10.1080/19443994.2016.1167126

Maddodi SA, Alalwan HA, Alminshid AH, Abbas MN. Isotherm and computational fluid dynamics analysis of nickel ion adsorption from aqueous solution using activated carbon. *South African Journal of Chemical Engineering* 2020; 32: 5-12. https://doi.org/10.1016/j.sajce.2020.01.002

Madhura L, Kanchi S, Sabela MI, Singh S, Bisetty K, Inamuddin. Membrane technology for water purification.

Environmental Chemistry Letters 2018; 16(2): 343–365. https://doi.org/10.1007/s10311-017-0699-y

Mbamba KC, Tait S, Flores-Alsina X, Batstone DJ. A systematic study of multiple minerals precipitation modelling in wastewater treatment. *Water research* 2015; 85: 359–370. https://doi.org/10.1016/j.watres.2015.08.041

Mubarak NM, Khalid M, Walvekar R, Numan A. Contemporary Nanomaterials in Material Engineering Applications. *Springer International Publishing* 2021.

Nandita D, Praveen G, Vineet K, Shivendu R. Functionalized nanomaterials I fabrications. CRC Press 2021, ISBN: 9781351021623

Omer NH. *Water Quality Parameters.* Water Quality-Science, Assessments and Policy, Kevin Summers, IntechOpen 2019. https://doi.org/10.5772/intechopen.89657.

Onishi T. *Theoretical Chemistry for Advanced Nanomaterials: Functional Analysis by Computation and Experiment.* Springer Nature 2020. ISBN: 9789811500060

Patawat C, Silakate K, Chuan-Udom S, Supanchaiyamat N, Hunt AJ, Ngernyen Y. Preparation of activated carbon from Dipterocarpus alatus fruit and its application for methylene blue adsorption. *RSC Advances* 2020; 10(36): 21082-21091. https://doi.org/10.1039/D0RA03427D

Peirce JJ, Weiner RF, Vesilind PA. *Environmental Pollution and Control.* 4th Edition, Butterworth-Heinemann, 1998. ISBN: 9780750698993, 0750698993.

Prasad KY. *Sedimentation in Water and Used Water Purification.* In: Lahnsteiner J. (eds). Handbook of Water and Used Water Purification, Springer, Cham 2019. http://doi-org-443.webvpn.fjmu.edu.cn/10.1007/978-3-319-66382-1_2-1

Reddy DHK, Yun YS. Spinel ferrite magnetic adsorbents: Alternative future materials for water purification?. *Coordination Chemistry Reviews* 2016; 315: 90-111. https://doi.org/10.1016/j.ccr.2016.01.012

Sarma GK, Sen Gupta S, Bhattacharyya KG. Nanomaterials as versatile adsorbents for heavy metal ions in water: a review. *Environmental science and pollution research international* 2019; 26(7): 6245–6278. https://doi.org/10.1007/s11356-018-04093-y

Sharma S, Bhattacharya A. Drinking water contamination and treatment techniques. *Applied Water Science* 2017; 7: 1043–1067. https://doi.org/10.1007/s13201-016-0455-7

Stein CR, Bezerra MTS, Holanda GHA, André-Filho J, Morais PC. Structural and magnetic properties of cobalt ferrite nanoparticles synthesized by co-precipitation at increasing temperatures. *AIP Advances* 2018; 8(5). https://doi.org/10.1063/1.5006321

Wadhawan S, Jain A, Nayyar J, Mehta SK. Role of nanomaterials as adsorbents in heavy metal ion removal from waste water: A review. *Journal of Water Process Engineering* 2020; 33. https://doi.org/10.1016/j.jwpe.2019.101038

Wei C, Zhang F, Hu Y, Feng C, Wu H. Ozonation in water treatment: the generation, basic properties of ozone and its practical application. *Reviews in Chemical Engineering* 2017; 33(1): 49–89.

World Health Organization, Guidelines for Drinking-Water Quality, 4th Edition, Incorporating the First Addendum, Geneva, 10, Acceptability aspects: Taste, odour and appearance, 2017. https://www.ncbi.nlm.nih.gov/books/NBK442378/

Lin Y, Liu H, Hu L. LQR suppression of hopf bifurcation in hodgkin-huxley neurons. *NeuroQuantology* 2019; 17(2): 22-32.